

# Nondestructive Sensor Using Microwaves from a Laser Plasma

Hiroto NAKAJIMA, Yoshinori SHIMADA<sup>1)</sup>, Toshihiro SOMEKAWA<sup>1)</sup>,  
Masayuki FUJITA<sup>1)</sup> and Kazuo A. TANAKA

*Graduate School of Engineering and Institute of Laser Engineering, Osaka University, 2-1 Yamada-Oka, Suita, Osaka 565-0871, Japan*

<sup>1)</sup>*Institute for Laser Technology, 2-6 Yamada-Oka, Suita, Osaka 565-0871, Japan*

(Received 10 October 2008 / Accepted 15 December 2008)

Ground penetrating radar (GPR) is a nondestructive sensor technology for detecting underground objects. GPR requires large-aperture antennas to survey a remote location precisely because of the expansion of microwaves. We propose a laser-driven GPR (LGPR) that uses microwave radiation from a laser plasma to achieve remote sensing. LGPR is expected to provide good spatial resolution with a small antenna. We selected a subnanosecond laser pulse as a suitable radiator for LGPR (L-S band). Experimental results show that the LGPR system can detect aluminum disks buried in sand.

© 2009 The Japan Society of Plasma Science and Nuclear Fusion Research

Keywords: laser plasma, rf emission, nondestructive sensing, subnanosecond laser

DOI: 10.1585/pfr.4.003

Ground penetrating radar (GPR) is a well-known non-destructive sensor technology that uses microwave echoes to find objects underground and examine building structures [1, 2]. Recently, demand has increased for remote sensing technology for landmine detection. Conventional GPR is effective only at a close range, or near the detection area. This is because an increase in the distance between the GPR and the remote survey area increases the area irradiated by the microwave, which leads to a deterioration in the angular resolution of the GPR. The microwave beam width must be as narrow as possible to prevent such deterioration. A large-aperture antenna is typically necessary for forming the narrow beam — the beam width  $\theta_{1/2}$  [deg] can be approximated by  $70 \times \lambda/D$ , where  $\lambda$  is the wavelength of radiated microwaves [m] and  $D$  is the aperture length [m] [3, 4]. We propose a laser-driven GPR (LGPR) using microwaves radiated from a laser plasma [5]. LGPR does not require a large-aperture antenna to sense a remote location because it generates a laser plasma that acts as a microwave radiator adjacent to the survey area, which is equivalent to a transmission antenna close to the survey area.

Electromagnetic waves at various frequency ranges (from MHz to THz), radiate from laser-produced plasmas [6–13]. The radiation is caused by the following processes. An intense laser pulse creates a laser plasma. The generated electrons and ions are accelerated toward the outside of the plasma by thermal pressure or Ponderomotive forces. The light electrons receive greater acceleration than the heavy ions. Charge separations are induced in the plasma by different expansion speeds of electrons and ions, which excite the electric dipole moments. These flickering

electric dipole moments radiate electromagnetic waves. It was reported that the radiation frequency spectrum corresponded to the laser-pulse envelope [8, 13]. A subpicosecond laser pulse has an optimal duration for the terahertz range [8–11]. We chose a subnanosecond laser pulse as the optimal duration for L-S band (0.5–4 GHz), which is regarded as a suitable frequency range for the GPR [3]. In this article, the spectrum of the microwaves radiated from laser plasma created by a subnanosecond laser pulse was measured. Using a LGPR system with a subnanosecond laser pulse, aluminum disks ( $\Phi$  7, 15, and 26 cm) were detected under a layer of sand.

Figure 1 shows a schematic of the experimental setup of the LGPR system. The laser (wavelength: 800 nm; pulse duration: 0.2 ns; pulse energy: 140 mJ; and repetition: 10 Hz) was focused on a spot (diameter:  $\sim$ 1 mm) using a lens with 2000 mm focal length in air at atmospheric pressure. The laser intensity was  $\sim 8.9 \times 10^{10}$  W/cm<sup>2</sup>. An EMCO 3102 (a log-spiral antenna, frequency range: 1–10 GHz) and Tektronix DSA70404 (a high-speed digital oscilloscope, maximum frequency: 4 GHz) were used as the receiving antenna and a recorder, respectively. A low-noise amplifier (Keycom KAV-005060LN-M; frequency range: 0.5–6 GHz; and gain: 40 dB) was used. One-line scan measurements (scan length: 1 m; scan step: 2.5 mm) were performed with an automatic scanning mirror. Aluminum disks (7, 15, and 26 cm in diameter, 1 cm thick) were buried at the center of the track at a depth of 1 cm in dry sand (dimensions: 1.2 m  $\times$  0.8 m  $\times$  0.15 m). The relative permittivity of the sand was  $\sim$ 5. The receiving antenna was 0.8 m high and 1.5 m from the aluminum disks. To reduce the noise from the external environment, 32 signals were averaged at each laser spot.

author's e-mail: nakajima-h@ile.osaka-u.ac.jp

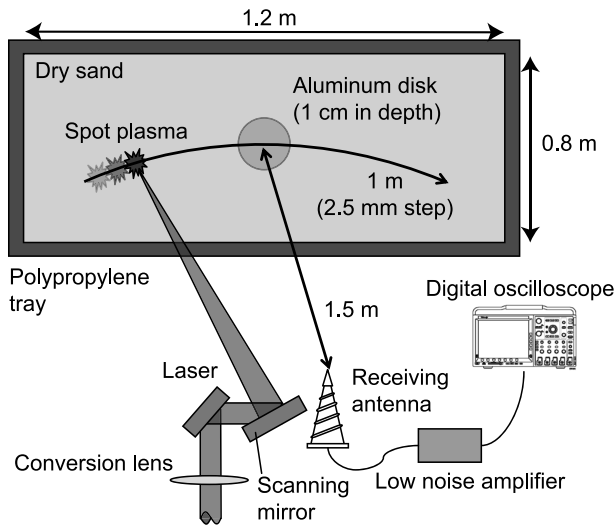


Fig. 1 Experimental setup of LGPR using a subnanosecond laser pulse.

Microwaves were measured with and without the production of the laser plasma. Figure 2 shows the spectrograms (window function: Hanning; window width: 80 ns; time step: 8 ns) of the measured data. The horizontal and vertical axes indicate the elapsed time [ns] and the radiated frequency [GHz], respectively. The amplitude is represented in 256-level grayscale from a maximum of 5 dB to a minimum of -20 dB. The time-dependent frequency spectra  $F(\omega, t)$  are derived from the measured data  $f(t)$  from  $t - 40$  to  $t + 40$  ns. Figure 2 (a) shows the result without the laser plasma, which is equivalent to the noise components from the laser oscillator. The noise components have a bandwidth from 0.3 to 0.7 GHz. Figure 2 (b) shows the spectrogram of the microwave radiated from the laser plasma, which was constructed by subtracting the noise components from the measured data with the laser plasma. The spectrum has a bandwidth from 1 to 3 GHz. This indicates that laser plasma produced by a subnanosecond laser pulse is suitable as a L-S band radiator. Note that the time duration of microwave radiation seems to be extended because of the window width (~50 ns). The inset shows the radiated waveform produced by the inverse Fourier transform of the signals shown in Fig. 2 (b). The horizontal and vertical axes indicate the elapsed time [ns] and the amplitude [V], respectively. The true duration can be estimated from this waveform at ~1 ns.

Figure 3 describes how the LGPR works in this experiment. Figure 3 (a) shows an experimental layout. The horizontal and vertical axes indicate the horizontal position,  $x$ , and the depth,  $z$ , respectively. The origin of  $z$  direction is at the sand surface. The Laser plasma ( $x = x_i$ ) radiates the microwave at  $t = 0$ . The radiated microwave penetrates the sand, is scattered by the buried object ( $x = x_{obj}, z = z_{obj}$ ), and arrives at the receiving antenna (dashed arrows) after

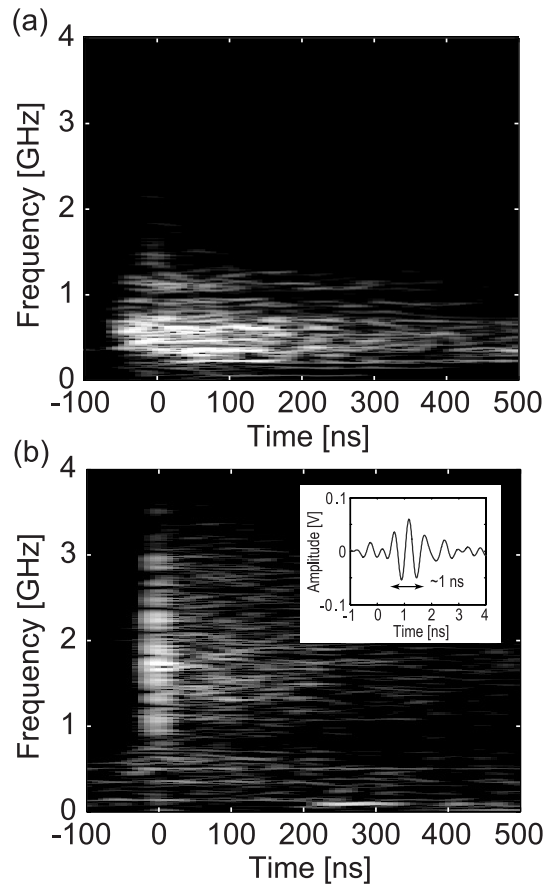


Fig. 2 Spectrograms of (a) noise components from the laser oscillator and (b) the microwave radiated from the laser plasma. The inset shows the radiated waveform produced by the inverse Fourier transform of the signals shown in Fig. 2 (b).

time  $t_s$ ,

$$t_s = \left\{ \sqrt{\epsilon_r} \left( \sqrt{(x_i - x_{obj})^2 + z_{obj}^2} + L_1 \right) + L_2 \right\} / c, \quad (1)$$

where  $L_1$  and  $L_2$  are the path length of the microwave propagating from the buried object to the sand surface and from the sand surface to the receiving antenna, respectively,  $\epsilon_r$  is the relative permittivity of the sand, and  $c$  is the speed of light. The path lengths,  $L_1$  and  $L_2$ , are constant because the buried object and the receiving antenna do not move.

Figure 3 (b) shows a B-scan [1, 2] image composed by directly arranging all the acquired data sets. The horizontal and vertical axes represent the horizontal position,  $x$ , and the elapsed time,  $t$ , respectively. The amplitude of the received signal is represented in grayscale in the B-scan image. The microwave echo reflected from the buried object, which is produced by the laser plasma ( $x = x_i$ ), is observed after  $t_s$ . Equation (1) indicates that the echoes reflected from a spot-shaped object should show a hyperbolic locus in the B-scan image. The shape and size of the underground object can be estimated from these loci. The methods described in Fig. 3 are well established in the conventional GPR scheme [1, 2].

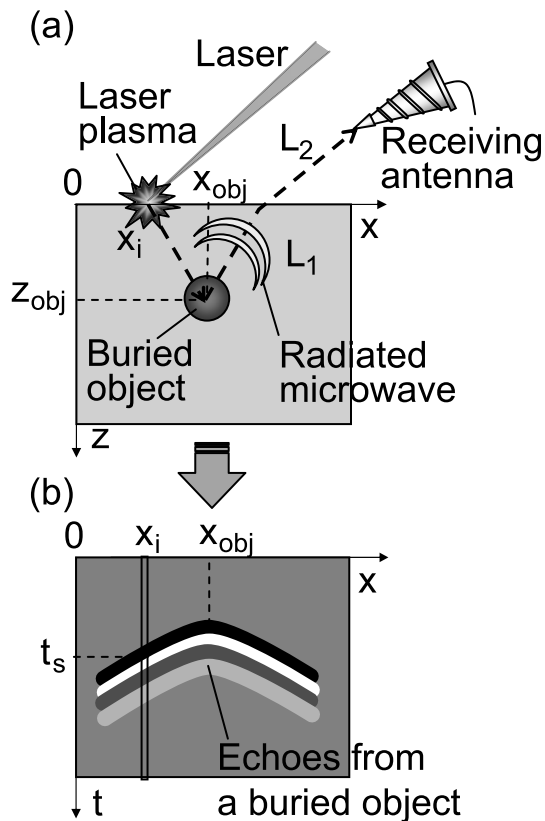


Fig. 3 Schematic describing LGPR (a) an experimental layout and (b) a B-scan image.

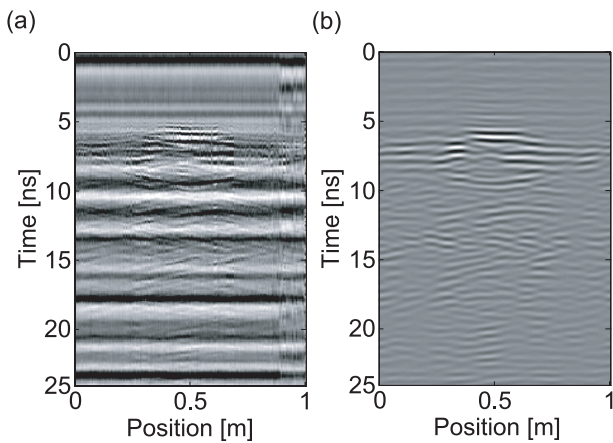


Fig. 4 (a) Raw and (b) f-k filtered B-scan images (a  $\Phi$  26 cm aluminum disk).

Figure 4 shows the measured data for a  $\Phi$  26 cm aluminum disk: (a) raw and (b) band-pass f-k filtered (frequency range: 1-3 GHz, wave number range:  $-10$ - $10$   $m^{-1}$ ) B-scan images [14]. The horizontal axis is the horizontal position,  $x$  [m], and the vertical axis is the elapsed time,  $t$  [ns]. Figure 4 was created using a 256-level grayscale image corresponding to the signals from a maximum of 50 mV to a minimum of  $-50$  mV. The raw scan data con-

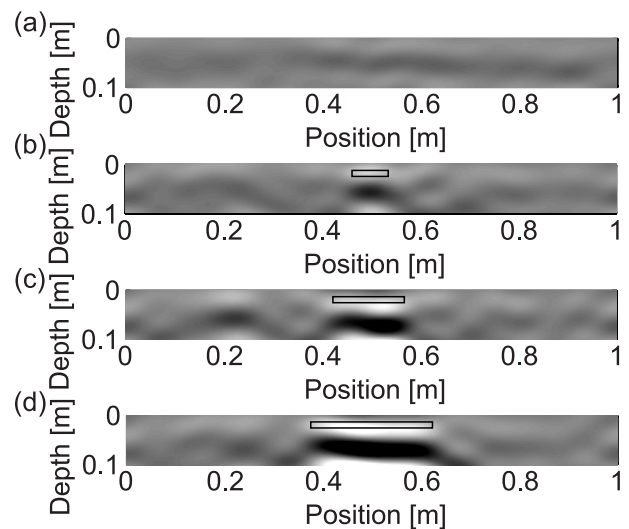


Fig. 5 Detection results of aluminum disks as B-scan images: (a) background, (b) 7 cm, (c) 15 cm, and (d) 26 cm in diameter. Each target buried at 0.5 m in the position and 0.01 m in depth.

tains the echoes reflected from the aluminum disk, noise components from a laser oscillator (low-frequency components: 0.3-0.7 GHz) and variation between laser shots. They are reduced by the band-pass f-k filter as shown in Fig. 4 (b).

Figures 5 (a)-(d) show the detection results of background and  $\Phi$  7, 15, 26 cm aluminum disks, respectively. The horizontal axis is the horizontal position [m], and the vertical axis is the depth [m]. They have been f-k filtered and clipped out as the part corresponding to the cross section of the sand. The depth was calculated from the elapsed time, accounting for the propagating velocity of the microwave and its origin at the sand surface. The rectangles in the figure represent the disk geometries. The constructed images clearly show the detection of aluminum disks and their size differences. The resolution was estimated at  $\sim 4$  cm (scan direction) from an envelope of the reflected echo. Here, the resolution is defined as the interval between two objects at which they can be distinguished by a threshold equal to half of their peak values.

In summary, we performed an experiment with LGPR using a subnanosecond laser pulse to create a spot plasma at  $9 \times 10^{10}$   $W/cm^2$  laser intensity. The radiated spectrum had the desired frequency (L-S band). Line-scan measurements (scan length: 1 m, scan step: 2.5 mm) by the LGPR were performed. The echoes reflected from each buried aluminum disk were observed clearly and showed the size difference. The scan resolution was 4 cm.

We appreciate the continual encouragement for this study given by Prof. K. Mima and Prof. C. Yamanaka.

[1] M. Skolnik, *Radar Handbook 3rd Edition* (McGraw-Hill books, New York, 2008).

- [2] D. Daniels, *Ground Penetrating Radar, 2nd Edition* (Peter Peregrinus Ltd, UK, 2004).
- [3] M. Bradley, T. Witten, M. Duncan and B. McCummins, Proc. SPIE **5415**, 421 (2004).
- [4] K. Kappra, M. Ressler, L. Nguyen and T. Ton, Proc. SPIE **3752**, 402 (1999).
- [5] H. Nakajima, M. Yamaura, Y. Shimada, M. Fujita and K.A. Tanaka, J. Phys.:Conf. Ser. **112**, 042086 (2008).
- [6] J.S. Pearlman and G.H. Dahlbacka, J. Appl. Phys. **49**, 457 (1977).
- [7] A. Ludmirsky, S. Eliezer, B. Arad, A. Borowitz, Y. Gazit, S. Jackel, A.D. Krumbein, D. Salzmann and H. Szichman, IEEE Trans. Plasma Sci. **13**, 132 (1985).
- [8] H. Hamster, A. Sullivan, S. Gordon, W. White and R.W. Falcone, Phys. Rev. Lett. **71**, 2725 (1993).
- [9] T. Bartel, P. Gaal, K. Reimann, M. Woerner and T. Elsaesser, Opt. Lett. **30**, 2805 (2005).
- [10] X. Xie, J. Dai and X.-C. Zhang, Phys. Rev. Lett. **96**, 075005/1-4 (2006).
- [11] K.Y. Kim, J.H. Glowonia, A.J. Taylor and G. Rodriguez, Opt. Express **15**, 8 (2007).
- [12] A.V. Kabashin, P.I. Nikitin, W. Marine and M. Sentis, Appl. Phys. Lett. **73**, 1 (1998).
- [13] F.S. Felber, Appl. Phys. Lett. **86**, 231501 (2005).
- [14] M. Sato, IEICE Trans. C, **Vol.J85-C**, No.7 p.520 (2002) [Japanese].